Petrochemical evidence for diversity of magma compositions at the northwestern Ethiopian volcanic province

Petrochemical evidence for diversity of magma compositions at the northwestern Ethiopian volcanic province

Agonafir Daniel Meshesha* and Ryuichi Shinjo*

*Graduate school of Engineering and Science, Department of Physics and Earth Sciences, University of the Ryukyus, Senbaru 1, Nishihara, Okinawa 903-0213, Japan

Abstract

Petrographic characteristics and whole-rock major and trace element data are presented for the Bure volcanic rocks from the northwestern Ethiopian plateau of East Africa continental flood basalt province, to investigate the processes that involved in the genesis of the erupted magma and its source composition during plume-induced continental rifting. The Bure area is mainly composed of stratified basalts, recent basalts, scoria cones and trachyte plugs. The successions of the erupted basalts are from transitional tholeiites to alkaline basalts. The transitional tholeiites have higher Zr/Nb (8.88-21.86) and Rb/Nb (0.66-1.87) than those of the alkaline (Zr/Nb=2.19-6.21, Rb/Nb=0.26-0.74), indicating that they are originated from distinct magma sources. The compositional variation in the transitional tholeiites cannot be explainable in terms of fractional crystallization of common (or similar) primary magma; instead it reflects the involvement of various mantle and crustal components in their petrogenesis. By contrast, the variation in the alkali suite can be explained by dominant fractional crystallization process of OIB-like primary basalts that derived from the Afar mantle plume. The strong lithospheric signature observed in the transitional tholeiites suggests pronounce interaction between the Afar plume and the lithosphere at the initial stage of continental break-up.

1. Introduction

The magmatism along the NNE-SSW running Ethio-Kenyan rift, the encircling plateaus and the Afar depression all together portray one of the largest and currently active igneous province in the East Africa (Fig. 1) and recognized as the East African Rift System (EARS). This 2,000 kilometer-long and widely distributed volcanic province is a result of lithospheric extension due to the domal uplift of the surrounding regions. Distribution and timing of magmatism and uplift of the entire area is accepted to be the

Received: June 30, 2004

result of an upwelling of anomalously hot mantle plume (Vidal et al., 1991), the Afar mantle plume (Mohr, 1967; Burke and Wilson, 1972; Gass, 1975; Berhe et al., 1987; White et al., 1989; Ebinger et al., 1998). Three mantle sources (old subcontinental lithospheric component, an HIMU-type plume component and a depleted mantle) were involved in the genesis of these continental flood basalts (CFBs), (e.g., Vidal et al., 1991; Stewart et al., 1996; Pik et al., 1998). However many authors have suggested that the east African CFBs suffered variable degree of crustal contamination (White et al., 1989; Vidal et al., 1991; Baker et al., 1996; Pik et al., 1998, 1999). Thus the role of mantle and crustal sources in their genesis still remains a subject of considerable debate.

Bure area is located at the western part of northwestern Ethiopian plateau of the East African CFB province (Fig. 1) where both pre-rift and post-rift basalts are widely distributed. Although Pik et al. (1998, 1999) reported detail geochemical data for the northwestern Ethiopia plateau, there is no such data for the Bure volcanic rocks.

In this paper, we present major and trace element data for basalts from the Bure area, to investigate the role of mantle and crustal sources in the genesis of the basalts and their association with the Afar mantle plume.

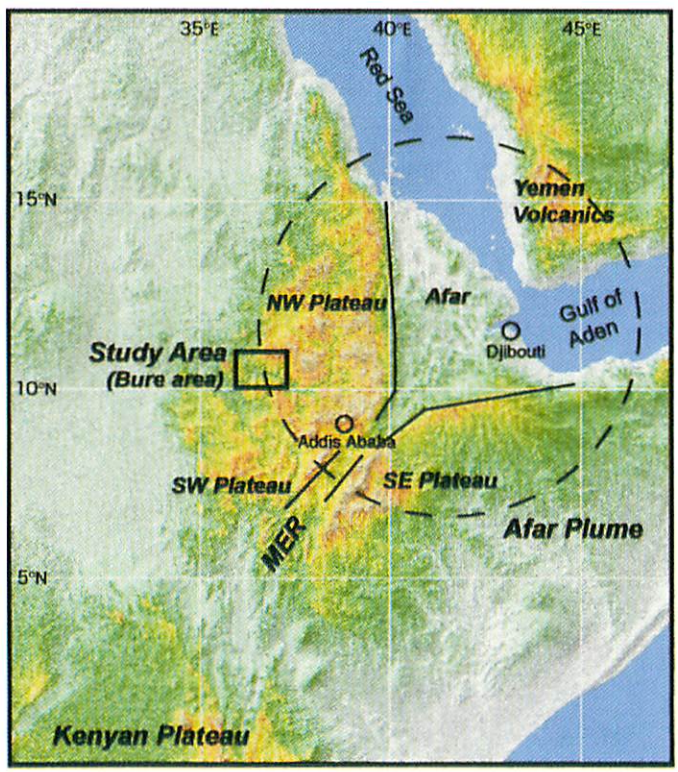

Fig. 1 Shaded relief map of East Africa and Arabia (NASA SRTM30) illustrating the position of the three rifts (Main Ethiopian Rift = MER, Gulf of Aden and Red Sea), as well as the Ethiopian and Yemeni plateaus which surround the Afar depression. The location of our study area is also indicated.

2. Regional Geology and Geological settings

The Ethiopian volcanic province is composed of Tertiary (Trap series) and Quaternary (Aden series) basaltic piles (Mohr, 1963) with thickness varying from 700 to 2,000 m at the plateau-rift margins (Brehe et al., 1987) and about 300,000 km^3 by volume (Mohr, 1963; Tefera et al., 1996). This volcanic province is subdivided into three major parts in terms of their geographical locations (Fig. 1). These includes the Ethiopian plateaus (the northwestern, southwestern, and southeastern plateaus), Main Ethiopian Rift (MER) and the Afar Rift (Kazmin, 1979; Berhe et al., 1987). Though the post-rift volcanism has been mainly concentrated along the axis of MER, it occurred at the Tana graben in NW plateau region (Kazmin, 1972; 1979) and also along the Yerer to Tulu-Wellel volcano-tectonic lineament between the northwestern and southwestern plateaus (Abebe et al., 1998).

The plateau regions display sub-horizontal successions of pre-rift flood basalts. It covers an area of several hundred kilometers across on the plateaus either side of the MER; the basalts along the southeastern plateau are relatively less voluminous compared to its counter part (Zanettin et al., 1980a). In general, the succession of erupted basalts starts with alkaline basalts to transitional tholeiitic basalts and then to alkaline basalts (Kazmin, 1980).

Volcanisms in the Ethiopian plateau were episodic and concentrated in 30 Ma and 22-12 Ma; young, more confined volcanoes have also formed after a major episode of flood basalts (Stewart et al., 1996). The occurrence of the latest stage volcanism outside the MER might be related to the development of new rift and fracture zones (Davidson et al., 1980). The surface tectonic expressions on the plateaus are not elaborated well, though micro to mega scale east-west and rift trend faults are appreciable in the region.

The volcanic rocks of northwestern part of Ethiopian plateau including the area studied in this paper are predominantly consists of Ashange Formation, Tarmaber Gussa Formation and Plateau basalts (Tefera et al., 1996). The Bure area is covered by Precambrian basement and various Cenozoic volcanic rocks (Fig. 2). The Cenozoic volcanic rocks cover more than half of the area and the thickest succession of the rocks are concentrated to the northeast part of the area.

3. Petrography of volcanic rocks from the Bure area

Samples were randomly collected from 30 outcrops according to their stratigraphic positions. The petrographic characteristics for these rocks are summarized in Table 1. The Cenozoic volcanic rocks from the area show a wide spectrum of compositional variations with respect to phenocryst distributions. The volcanic rocks are classified based on mode of occurrence, petrochemical composition and stratigraphic positions. These include stratified basalts, recent basalts, scoria cones and trachyte plugs.

3.1 The stratified basalts

The oldest volcanic rocks in the Bure area are the stratified basalts (Fig. 2). Two fold sub-divisions into lower and upper basalts are proposed for these basalts, based on geomorphological features and the relative stratigraphic position; the lower basalts are transitional tholeiites basalts whereas upper basalts are alkaline basalts. The petrographic study shows that petrographically variable layers stratified in each stratigraphic sequence (Table 1).

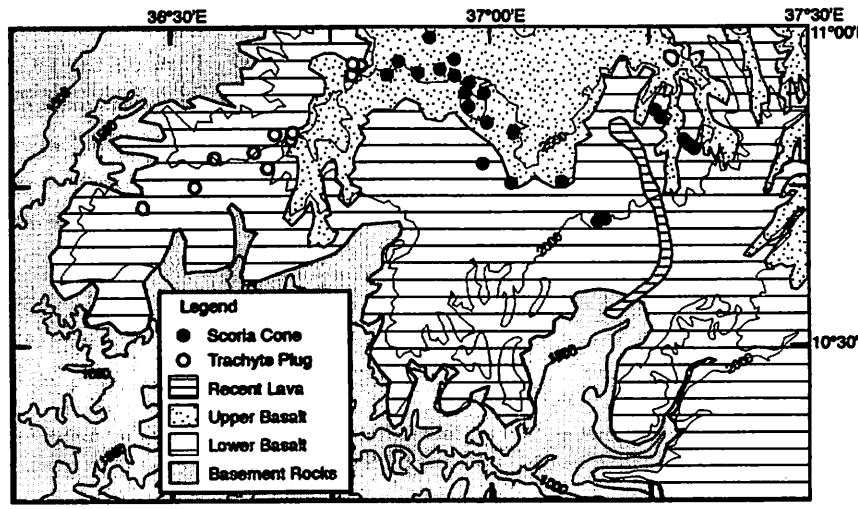

Fig. 2 Simplified geological map of the Bure area. Topographic contour lines (interval = 500 m) are also indicated. Basement rocks include Precambrian gneisses, lowgrade rocks and granitoids. Stratified basalts are divided into the lower and upper basalts.

Table 1. Lithological and petrographic characteristics of the Bure volcanic rocks

	Rock type	Texture	Mineral assemblage		
			Phenocrysts	Groundmass	Alteration/Remark
Trachyte plugs	Trachyte	Trachytic	San	Plag + San + Pxn (trace) (Holocrystalline)	San limonitized, trace quartz
Recent basalt	Vesicular Oliv-Phyric basalt	Intergranular	Oliv	Plag + Oliv + Pxn + Opq. (Hypohyaline)	vesicles about 15 % by volume
Upper basalts	Aphyric basalt	Trachytic	Pxn	Plag + Pxn + Opq. (Holocrystalline)	Pxn highly altred, Plag strongly aligned, trace quartz
	Plag-phyric basalt	Trachytic Intergranular	Plag Oliv	Plag + Oliv +Pxn +Opq. (Holocrystalline)	Plag strong alignment, oliv altered to iddingsite, corona tex.
	Oliv-phyric basalt	Trachytic Intergranular	Oliv Plag Pxn	Plag + Oliv + Pxn +Opq. (Hypocrystalline)	Plag show alignment, Oliv altered along the fracture to iddingsite & show mimic tex., Pxn altered along rim
Lower basalts	Pyrn-phyric basalt	Subophitic Intergranular	Pxn Plag	Plag + Oliv + Pxn +Opq. (Holocrystalline)	Oliv altered to iddingsite, Pxn altered, Plag show zonning
	Oliv-phyric basalt	Intergranular Pilotaxitic	Oliv Plag Pxn	Plag + Oliv + Pxn +Opq. (Holocrystalline - -Hypocrystalline)	Oliv show corona tex, altered to Iddingsite, Pxn altered
	Aphyric basalt	Trachytic Intergranular	Plag	Plag + Oliv + Pxn +Opq. (Holocrystalline)	Plag altered
	Plag-phyric basalt	Trachytic Intergranular	Plag Pxn trace Oliv	Plag + Oliv +Pxn +Opq. (Holocrystalline)	Plag show minor zonning, some Pxn alterd & show corona tex.

Abbriavations Plag=Plagioclase; Pxn=Pyroxene; Oliv=Olivine; San=sanidine; Opq=Opaque minerals; tex=texture

Lower basalts

The Lower basalts have the lowest stratigraphic position exposed throughout the area (Fig. 2). The maximum thickness is about 900 m at the north-central part of the area with pronounced vertical variations. In the lower basalt section, the rock occupying the lowest part is deeply weathered and irregularly jointed. They unconformably overlie the Precambrian basements (Seyid et al., 2003; Gerra et al., 2003), and are conformably overlain by other flows or strata that are relatively less weathered and crushed. To the west and east part of the area, there are minor intercalation of pyroclastic rocks (Seyid et al., 2003; Demisse et al., 2003). The lower basalts are porphyritic to aphyric with phenocrysts of plagioclase, pyroxene, and olivine. Holocrystalline groundmass is composed of variable proportion of plagioclase, olivine, pyroxene (sometimes, two pyroxenes) and opaque minerals (Fe-Ti oxides). In hand specimen, the rock is mostly dark gray, light gray and sometimes blush gray with weathered pink to pinkish gray surface. The secondary minerals are iddingsite, minor calcite, zeolite and quartz. The lower basalts can be divided into four main groups on the basis of phenocryst mineral assemblages (Table 1). It has thick strata of interstratified plag-phyric, oliv-phyric, pxn-phyric, and aphyric basalts of variable thickness.

Upper basalts

The Upper basalts occupy stratigraphically upper position in the region and conformably overlie the lower basalts. It has about a maximum thickness of 600 m at the northeastern part of the area. They form cliffs and are unevenly distributed patchy outcrops in the area (Fig. 2). There is about 5 m thick reddish clay soils (paleosoils) between the lower and upper basalts at the Wange quarry section and along the main road between Angut Michael and Yechereka town (Demisse et al., 2003). Rocks are aphyric to porphyritic in texture. Groundmass is generally holocrystalline with variable proportion of plagioclase, olivine, pyroxene, and opaque minerals. In hand specimen, the rocks are mostly dark gray color. The secondary minerals are iddingsite, minor calcite, zeolite, and quartz. The upper basalt can be divided into three main groups; on the basis of phenocryst mineral assemblages (Table 1). It is composed of interstratified plag-phyric, oliv-phyric, and aphyric basalts of variable thickness.

3.2 Recent basalts

The olivine-phyric gray to dark gray lava flow occurs along small graben-like features in the northeastern part of the studied area (Fig. 2). Since the lava covers the Quaternary loose sediments, its activity seems to be recent. Observation of ropy surface indicates flow direction from the north to south. Lava is vesicular and pahoehoe type flows (Demisse et al., 2003; Gerra et al., 2003) with blister structure (Worku et al., 2003; Gerra et al., 2003). The vesicles are stretched and aligned in the N-S direction, their

distribution decreases towards the base of the flow. Basically, the vesicles are not filled. The lava contains olivine (<10%) as phenocryst in holocrystalline groundmass (Table 1).

3.3 Scoria cones

The scoria cones form spatter cones throughout the north central part of the area (Fig. 2). The majority of the cones are aligned in NW-SE direction (Demisse et al., 2003) along certain lineaments and sometime it forms isolated cones and half-breached morphology (Gerra et al., 2003). These cones are well preserved and the rocks are mostly unaltered. In hand specimen, scorias are brown to pink, characterized by poorly to moderately sorted and loose grains of lappilli to bomb size of different shape such as rod, spindle, etc (Gerra et al., 2003). The rock fragments are mainly olivine to olivine-pyroxene phyric basalts with secondary minerals (zeolite and calcite) and olivine-pyroxene nodules (Demisse et al., 2003; Gerra et al., 2003).

3.4 Trachyte plugs

The trachyte plugs have intruded the lower and upper basalts. They mainly occupy the northwestern part of the area with NE-SW alignment (Fig. 2). They form upright slab which is columnarly jointed and developed cliff in all sides (Gerra et al., 2003). In hand specimen, they are light gray to greenish gray and porphyritc. The average composition shows that it is composed of sanidine as phenocrysts in holocrystalline groundmass (Table 1).

4. Analytical methods

Representative samples from all rock types, except for scorias, were crushed into mm-sized chips; the freshest rock chips carefully hand picked under streo-microscope were pulverized using alumina ceramic swing mill. The whole-rock major and trace elements (Ba, Ce, Co, Cr, Nb, Ni, Pb, Rb, Sr, Th, V, Y, and Zr) were determined on the fused glass beads by using X-ray fluorescence spectrometry (Shimadzu XRF-1800) at the Department of Physics and Earth Sciences, University of the Ryukyus. The glass beads were prepared by fusing 1 (±0.0005) g of rock powder mixed with 5 (±0.0010) g of lithium tetraborate. Reproducibility and accuracy of the XRF analyses were checked using the international rock standards (JB-1, BCR-1, and BHVO-2) (Table 2). Accuracy for major oxides are mostly better than 3%; those of trace elements are slightly worse (generally <10%).

5. Geochemical Results

Whole-rock major and trace elements data for representative samples from the Bure area are listed in Table 3.

Table 2 Data for three international rock standards compared with reference values

Standards	JB-1			BCR-2			BHVO-2		
	Reference value	This study (n=3)	Accuracy	Reference value	This study (n=3)	Accuracy	Reference value	This study (n=3)	Accuracy
SiO_2 (wt%)	52.37	52.65	0.5%	54.1	53.71	−0.7%	49.9	49.88	0.0%
TiO_2	1.32	1.319	−0.1%	2.26	2.33	3.1%	2.73	2.73	0.0%
Al_2O_3	14.53	14.49	−0.3%	13.50	13.31	−1.4%	13.5	13.41	−0.7%
Fe_2O_3	8.99	9.54	6.1%	13.80	13.79	−0.1%	12.3	12.57	2.2%
MnO	0.153	0.152	−0.7%	0.196	0.199	1.5%	0.167	0.165	−1.2%
MgO	7.71	7.67	−0.5%	3.59	3.45	−3.9%	7.23	7.01	−3.0%
CaO	9.25	9.26	0.1%	7.12	7.03	−1.3%	11.4	11.38	−0.2%
Na_2O	2.77	2.73	−1.4%	3.16	3.08	−2.5%	2.22	2.20	−0.9%
K_2O	1.434	1.41	−1.7%	1.79	1.77	−1.1%	0.52	0.52	0.0%
P_2O_5	0.255	0.257	0.8%	0.35	0.349	−0.3%	0.27	0.267	−1.1%
Total	98.78	99.48	0.7%	99.87	99.02	−0.8%	100.24	100.13	−0.1%
Ba (ppm)	493	525	6.6%	683	729	6.7%	130	131	0.8%
Ce	68	68	0.3%	53	59	10.7%	38	40	4.4%
Co	38	33	−14.5%	37	36	−2.7%	45	38	−16.3%
Cr	425	435	2.4%	18	22	20.4%	280	255	−8.9%
Nb	35	38	9.9%	13	12	−11.0%	18	15	−14.3%
Ni	133	141	6.0%		10		119	106	−10.6%
Pb	7.1	7	−1.4%	11	10	−12.1%		2	
Rb	41.3	40	−3.0%	48	42	−12.1%	9.8	11	7.9%
Sr	444	458	3.2%	346	314	−9.3%	389	376	−3.3%
Th	9.3	9	−6.8%	6.2	5	−19.4%	1.2	1	10.8%
V	211	211	0.0%	416	420	1.0%	317	307	−3.2%
Y	24.3	23	−6.3%	37	32	−12.8%	26	25	−5.4%
Zr	141	144	2.1%	188	169	−9.9%	172	164	−4.7%

Table 3 Major and trace element compositions of volcanic rocks from the Bure area

Type	Lower basalts													Upper basalts	
Sample No	TD-1228A	TD-1202	TD-1239	ASW-503	TL-208	TL-229	TL-253	EH-235A	AN-201	MH-4510A	MH-4521	WH-3496	TN-28	TD-1034B	SM-172
SiO_2(wt.%)	50.56	51.62	46.93	51.39	52.85	50.11	48.90	48.52	47.01	49.18	49.50	47.07	43.20	46.84	47.21
TiO_2	2.441	1.706	1.260	2.312	2.231	2.092	2.306	2.126	1.252	3.500	3.544	3.723	3.894	3.142	2.505
Al_2O_3	13.88	14.47	14.29	14.24	14.20	15.63	14.44	15.92	15.53	13.11	13.99	13.88	14.18	16.46	16.72
Fe_2O_3	13.91	11.94	11.62	13.39	12.21	12.9	13.74	11.98	11.98	16.51	13.27	14.04	13.39	14.48	12.90
MnO	0.21	0.17	0.18	0.18	0.19	0.19	0.19	0.18	0.18	0.24	0.22	0.21	0.19	0.21	0.18
MgO	5.00	6.05	11.14	5.29	3.77	5.16	5.79	6.56	8.65	3.89	4.73	6.05	8.34	4.38	5.39
CaO	9.67	10.44	9.64	8.98	6.76	10.83	11.04	10.69	10.48	8.59	8.77	10.26	10.34	6.60	7.91
Na_2O	2.94	2.71	2.89	2.86	3.36	2.56	2.62	2.62	2.14	2.94	3.07	2.77	2.79	3.82	3.71
K_2O	0.62	0.44	0.64	0.94	2.35	0.48	0.45	0.74	0.36	1.18	1.05	0.49	0.67	1.39	1.00
P_2O_5	0.214	0.130	0.197	0.268	0.807	0.176	0.197	0.229	0.114	0.416	0.811	0.808	0.568	0.532	0.585
LOI	0.46	0.34	0.35	2.46	1.22	0.72	0.93	2.07	3.42	0.87	1.18	0.87	2.89	1.88	1.24
Total	99.90	100.02	99.14	102.31	99.94	100.85	100.60	101.64	101.12	100.43	100.13	100.17	100.45	99.73	99.35
Ba (ppm)	134	149	236	308	1665	132	86	194	754	232	797	799	476	569	426
Ce	30	32	18	55	120	18	21	30	8	62	69	57	71	67	64
Co	42	39	60	43	29	39	44	39	46	38	34	39	46	41	44
Cr	23	71	457	45	19	56	45	184	326	19	48	61	241	10	21
Nb	7	6	22	10	18	7	10	13	4	19	18	14	57	36	30
Ni	22	32	283	63	12	29	46	100	134	12	12	30	83	3	20
Pb	5	4	2	4	12	4	2	4	3	7	6	5	3	5	6
Rb	14	8	14	18	28	13	9	13	8	24	18	13	15	23	17
Sr	264	257	333	351	742	299	272	337	350	264	560	677	740	520	556
Th	1	3	3	2	3	2	2	4	0	5	4	2	3	2	2
V	392	263	191	310	227	368	372	345	251	397	338	353	302	162	169
Y	31	27	22	33	38	26	25	25	21	42	31	25	24	33	31
Zr	145	114	90	181	317	127	130	154	94	222	158	133	230	226	182

LOI, loss on ignition; Fe_2O_3, total Fe_2O_3

Table 3 (Continued)

Type	Upper basalts								Recent basalts		Trachyte plugs		
Sample No	SM-120	SOG-3136	SOG-3061B	SOG-3104	TN-85	SOG-3091	SOG-3005	SOG-3043	TD-1003	SOG-3157	TD-1136A2	TD-1135B	SM-113
SiO_2 (wt.%)	49.68	44.55	58.31	57.58	49.99	44.75	44.37	45.72	46.56	48.54	64.01	63.91	63.98
TiO_2	2.260	2.978	1.009	0.428	2.167	3.735	2.430	1.931	1.743	1.755	0.171	0.174	0.407
Al_2O_3	16.97	15.72	18.32	18.09	15.20	15.09	12.52	14.72	14.91	16.77	17.09	17.01	15.85
Fe_2O_3	10.43	13.03	4.75	6.12	12.52	14.88	11.50	11.00	10.91	11.72	4.11	4.00	4.44
MnO	0.21	0.19	0.23	0.38	0.18	0.23	0.17	0.18	0.17	0.16	0.14	0.09	0.19
MgO	4.28	7.96	1.06	0.90	4.66	4.87	12.01	9.63	10.05	6.14	0.08	0.05	0.16
CaO	6.32	8.88	2.93	1.72	9.10	8.05	11.53	10.14	10.27	10.42	0.40	0.59	0.34
Na_2O	4.32	3.09	6.62	6.78	3.38	3.52	2.05	3.97	3.01	3.28	6.78	6.8	7.31
K_2O	2.40	0.98	3.96	4.87	0.93	1.86	0.82	1.47	1.17	1.00	5.36	5.49	5.05
P_2O_5	1.027	0.599	0.240	0.241	0.278	0.907	0.379	0.495	0.293	0.279	0.038	0.068	0.046
LOI	2.02	2.06	1.34	1.63	1.77	2.28	2.60	0.36	0.14	0.67	0.77	0.99	0.75
Total	99.92	100.04	98.77	98.74	100.17	100.18	100.39	99.61	99.22	100.74	98.95	99.17	98.53
Ba (ppm)	945	354	1516	883	318	624	325	593	366	347	162	123	32
Ce	120	68	140	198	57	109	40	72	43	50	320	354	338
Co	21	52	6	8	41	37	54	45	51	34	4	4	4
Cr	16	27	5	7	20	18	767	315	321	158	6	5	8
Nb	76	36	128	195	22	81	30	75	32	26	176	182	356
Ni	8	79	8	6	20	5	255	187	184	51	16	13	11
Pb	5	4	8	11	5	4	3	4	2	4	12	13	20
Rb	46	18	89	119	18	59	19	43	24	18	123	145	193
Sr	1133	601	1077	268	425	927	432	733	518	518	14	14	19
Th	6	3	9	15	4	5	4	6	2	3	15	15	29
V	149	233	17	4	340	168	284	199	227	219	4	3	6
Y	26	28	29	30	28	29	22	20	17	22	90	83	50
Zr	231	188	312	427	198	304	163	169	135	133	1072	1144	944

5.1 Major elements

The total alkali-silica classification diagram of the Bure volcanic rocks comprises two chemically distinct suites (Fig. 3): alkali basalts (basanite, basalt, trachybasalt, basaltic trachyandesite and trachyte) and transitional tholeiitic basalts (basalt and basaltic trachyandesite). Trachyte plugs and recent basalts fall in the alkali trachyte and basalt fields, respectively.

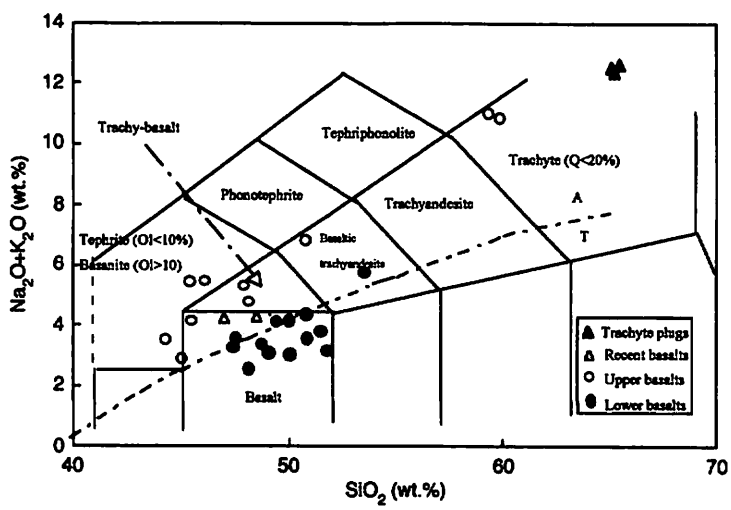

Fig. 3 Total-alkali vs. silica diagram of the Bure volcanics (Le Maitre et al., 1989). The Tholeiitic (T)-alkaline (A) divide is shown (Irving and Baragar, 1971).

In MgO against SiO_2 plots, the MgO content varies from 0.05 wt. % in trachyte to 12 wt. % in alkali basalts; most of the value concentrated below 6 wt. % (Fig. 4), suggesting their fractionated nature.

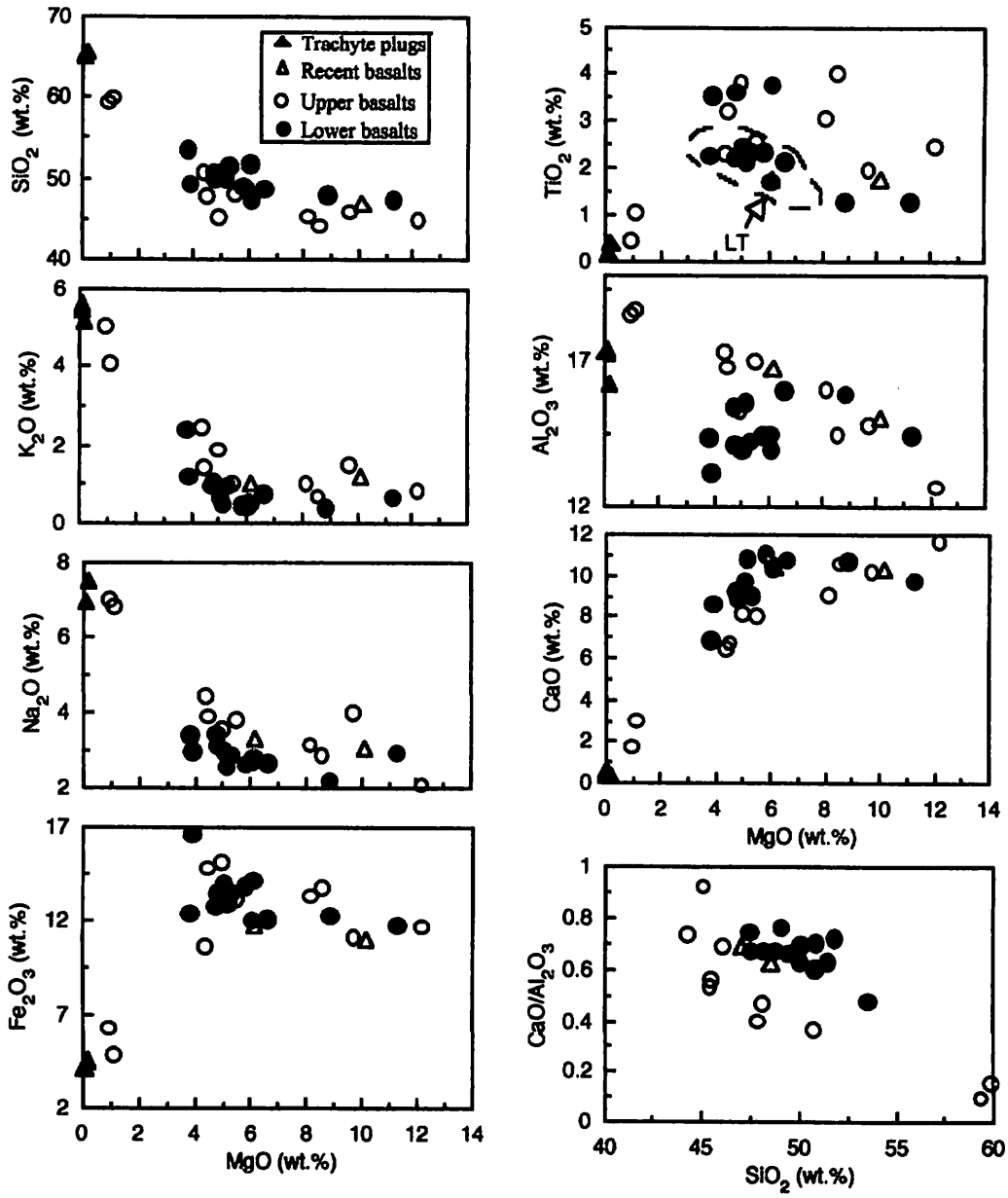

Fig. 4 Selected major elements against differentiation index (as MgO) diagrams of the Bure volcanics. The dashed line in TiO_2-MgO plot indicates the field of NW Ethiopian Low-Ti (LT) magma type flood basalts (Pik et al., 1998; 1999).

In the selected oxides vs. MgO variation diagram (Fig. 4), the two volcanic suites display increase in SiO_2, Na_2O, and K_2O with decreasing MgO contents. Al_2O_3 increase with decreasing MgO in alkaline suite, whereas Al_2O_3 in transitional tholeiitic suites positively correlate with MgO; at higher MgO both suites have the same trend. CaO tends to decrease at less than 6 wt. % MgO. TiO_2 contents negatively correlates with MgO in transitional tholeiitic suite, whereas TiO_2 contents are scattered in alkali suite. Some basalts fall in the field of Low-Ti type basalts (defined by Pik et al., 1998; 1999), but others have slightly higher TiO_2 contents. The recent basalts and trachyte plugs mainly follow the alkali suite trends.

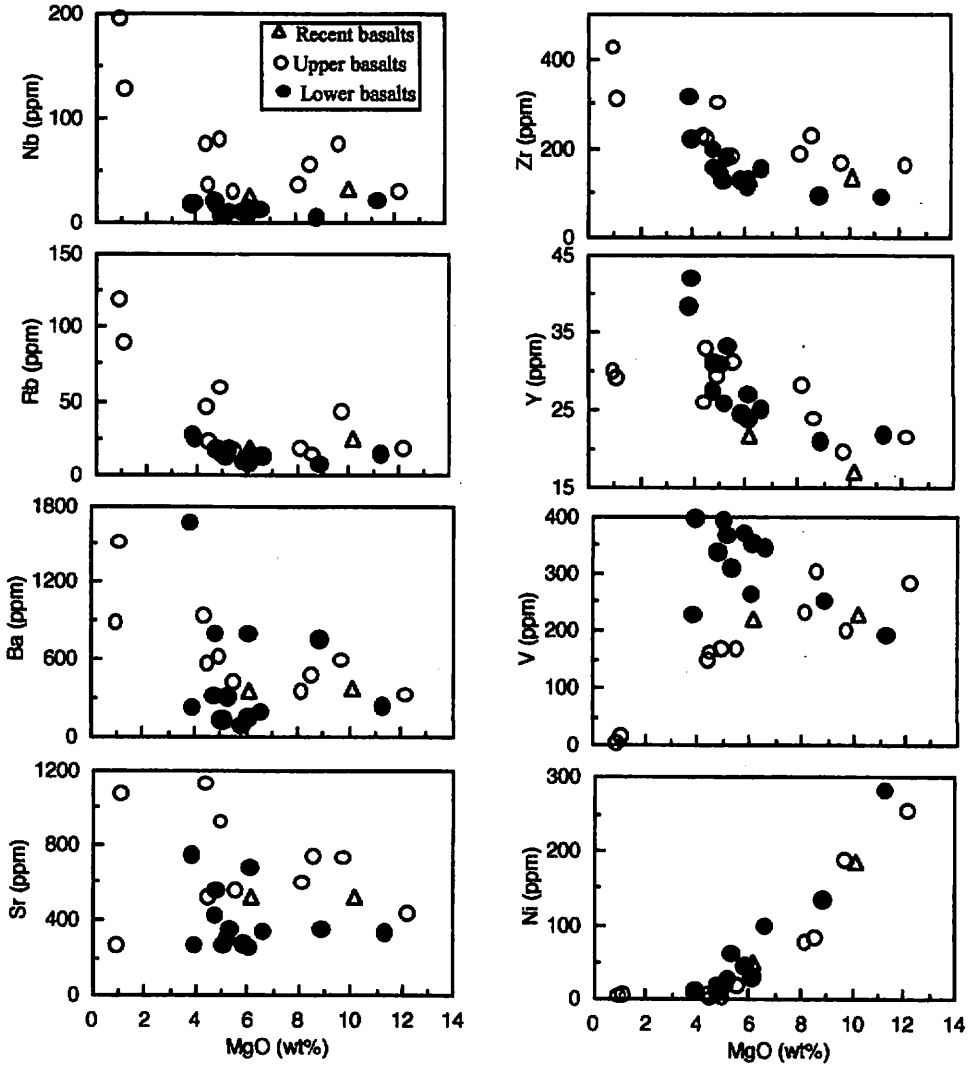

Fig. 5 Selected trace elements against differentiation index (as MgO) diagrams of the Bure volcanics.

5.2 Trace elements

The variations of the two suites are also well expressed in MgO against selected trace element diagrams (Fig. 5). Ni shows positive correlation with MgO, suggesting olivine fractionation. V is negatively correlated with MgO contents in transitional tholeiite suite, while positive trend is observed for alkaline suite. Nb, Zr, Y, and Rb increase with decreasing MgO. Sr and Ba show scattered pattern in both suites.

Primitive mantle-normalized multi-element diagrams of the Bure volcanic suites display two distinct patterns with respect to large ion lithophile elements (LILE), Nb and Th (Fig. 6). The transitional tholeiitic basalts (lower basalts) have flat patterns with slight negative anomalies of Nb and positive Pb anomalies, broadly similar to intra-plate tholeiite pattern. The alkali suite (upper and recent basalts) shows typical OIB-like patterns enriched in LILE relative to high field strength elements (HFSE) with Ba-Nb-Pb peaks and Th-Ce trough. Trachyte plugs have irregular patterns enriched in LILE with pronounced negative anomalies in Ba, Sr, P, and Ti (Fig. 6).

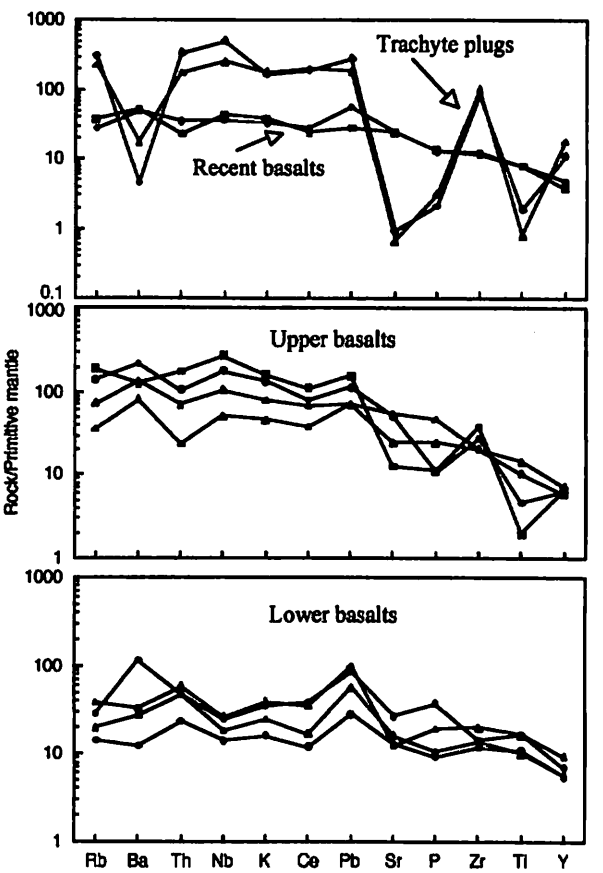

Fig. 6 Primitive mantle-normalized multi-element diagrams for representative basalts of the Bure volcanics. Primitive mantle values are from Sun and McDonough (1989).

6. Discussion

The major and trace element variation diagrams show two distinct trends for transitional tholeiites and alkaline basalts (Figs. 4 and 5). The two trends are also attested in the plot of SiO_2 against CaO/Al_2O_3 (Fig. 4). The decreases in CaO/Al_2O_3 in alkali basalts are accompanied by an increase in incompatible trace element abundance (Fig. 5) and fractionation (Fig. 3). Thus, these two variation trends can be inherited from compositionally different magma sources.

The plots of Zr vs. Zr/Nb and Rb vs. Rb/Nb display two distinct trends: one with flat-gentle slope (alkali basalts) and the other with steep-vertical slope (transitional tholeiites) (Fig. 7). Since incompatible element ratios do not significantly vary on fractionation and partial melting processes, these deviations in Fig. 7 clearly indicate that the two suites have different petrogenesis and that fractional crystallization and partial melting of common source cannot explain these deviations. The transitional tholeiitic basalt suite has heterogeneous incompatible element ratios, which can be explained by either source heterogeneity or crustal contamination. Therefore the strong lithospheric signature in the genesis of transitional tholeiitic basalts can be explained by the involvement of lithospheric mantle-derived melts or crustal contamination of asthenospheric mantle. In contrast, the alkali basalts have nearly constant Zr/Nb and Rb/Nb with increasing Zr and Rb contents, which indicates that compositional diversity in alkaline basalts can be accounted for by fractional crystallization of primary magma.

The transitional tholeiitic suite has higher Zr/Nb and Rb/Nb than the alkali suite (Fig. 7). The greatest variation in these ratios is observed in transitional tholeiitic suite. However the alkali suite does not show such pronounced variation; their ratios fall in OIB compositional range, suggesting that the sources for alkali basalts may be located in the deep mantle.

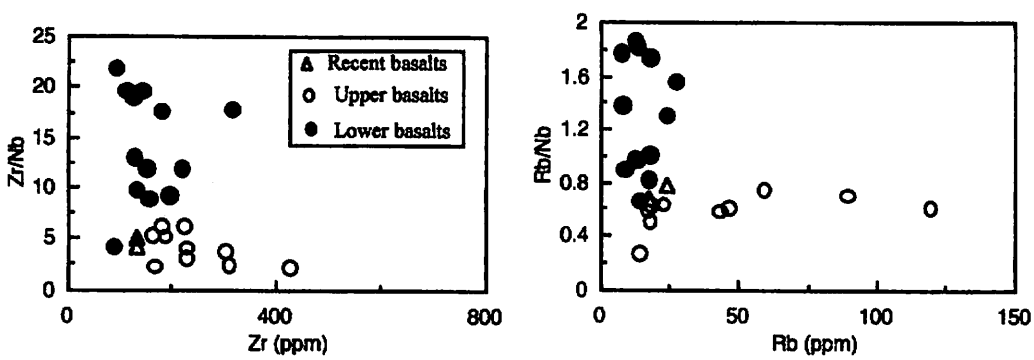

Fig. 7 Plots of selected incompatible trace element ratios against trace element contents of the Bure volcanics.

In the diagrams of Nb/Zr against Rb/Zr and Ba/Zr, (Fig. 8) the mantle-crust interactions are clearly demonstrated. The alkaline basalts (Upper and Recent basalts) show an enrichment of Nb, Ba and Rb and most of the data are plotted along the mantle array of OIB and within-plate alkaline (WP-alk) basalts. It is characterized by higher Nb/Zr and Rb/Zr with relatively lower value of Ba/Zr ratios. The alkaline basalts do not show any interaction with the crustal contaminant. Therefore, as shown in Fig. 7 fractional crystallization is the dominant process for compositional variation in the alkali suite. On the other hand, the transitional tholeiites (Lower basalts) are characterized by the depletion of Nb and Rb with variable Ba and have lower Nb/Zr and Rb/Zr with relatively wider value of Ba/Zr. The transitional tholeiite basalts are displaced from the E-MORB, WP-th and PM basalts fields (Fig. 8) and outspread towards the crustal contaminant (East Africa, Lower and Upper crust); their high Ba/Zr reflect the involvement of other components having high Ba/Zr (i.e., crustal component) in their petrogenesis.

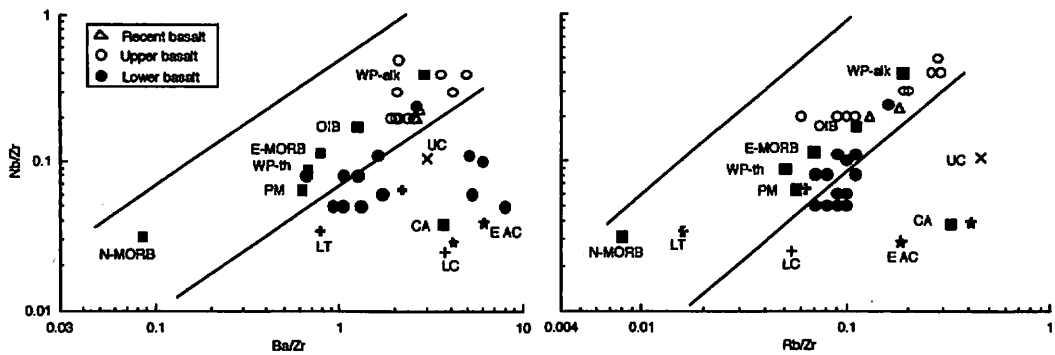

Fig. 8 Plots of selected incompatible trace element ratios of the Bure volcanics. Also shown representative basalts from valious tectonic settings: Within-plate tholeiite (WP-th), within-plate alkali basalts (WP-alk) and calc-alkaline (CA) values from Pearce (1982). Oceanic island basalt (OIB), E-type MORB (E-MORB), N-type MORB (N-MORB), and primitive mantle (PM) basalts values from Sun and McDonough (1989). East Africa Crustal value (EAC) and low-Ti type basalts (LT) values from Pik et al. (1999). Upper (UC) and lower (LC) continental crust values from Taylor and McLennan (1981).

7. Conclusions

The Bure volcanic rocks are composed of two distinct volcanic suites: transitional tholeiitic and alkali basaltic suites. The eruptive sequence is from voluminous transitional tholeiite (lower) to alkaline (upper) in the plateau-forming stage, which is followed by the minor amount of alkaline basalts (recent basalts and scorias) and highly fractionated trachyte plugs.

The two suites show significant geochemical variations and they are originated by differentiation of compositionally distinct magmas. The trace element characteristics observed in transitional tholeiitic suite are variable with heterogeneous incompatible trace element ratios (e.g., Zr/Rb and Rb/Nb). They are derived from lithospheric mantle melt or crustal contamination of asthenospheric magma. The alkali suite has homogeneous incompatible trace element and displays OIB-like trace element characteristics, indicating that they were originated from OIB-like Afar plume source.

Acknowledgements

This work was supported by the Grants-in-Aid for Scientific Research (C) from the Ministry of Education, Culture, Sport, Science and Technology, Japan to R.S. (Subject No. 13640483). We thank T. Matsumoto (University of the Ryukyus) for reading the manuscript and Y. Kato (emeritas Professor, University of the Ryukyus) for encouragement.

References

Abebe, T., Mazzarini, F., Innocentti, F. and Manetti, P. (1998) The Yerer-Tullu Wellel Volcano-tectonic Lineament: A Transitional structure in Central Ethiopia and the Associated Magmatic activity. J. African Earth Sci., 26, 135-150.

Baker, J., Thirlwall, M. and Menzies, M. (1996) Sr-Nd-Pb isotopic and trace element evidence for crustal contamination of plume-derived flood basalts: Oligocene flood volcanism in western Yemen. Geochim. Cosmochim. Acta, 60, 2559-2581.

Berhe, S., Desta, B., Nicoletti, M. and Tefera, M. (1987) Geology, geochronology and geodynamic implications of the Cenozoic magmatic province in W and SE Ethiopia. J. Geol. Soc. London, 144, 213-226.

Burke, K. and Wilson, J. T. (1972) Is the African Plate Stationary? Nature, 239, 387-390.

Davidson, A. and Rex, D.C. (1980) Age of volcanism and rifting in southern Ethiopia. Nature, 283, 65-66.

Demisse, T. and Hailu, E. (2003) Geology of sub-sheet F, L and M (Bure, NC37-5). Regional Geology and Geochemistry Department, Geological Survey of Ethiopia, Addis Ababa, Ethiopia.

Ebinger, C. J. and Sleep, N. H. (1998) Cenozoic magmatism throughout east Africa resulting from impact of a single plume. Nature, 395, 788-791.

Gass, I.G. (1975) Magmatic and tectonic process in the development of the Afro-Arabia dome. In: "Afar Depression of Ethiopia". Eds A. PILGER and A. ROSLER, Schweizerbartsche Verl., Stuttgurt, 10-18.

Gerra, S., Mokonnen, S. and Niguse, T. (2003) Geology of sub-sheet C, D and E (Bure, NC37-5). Regional Geology and Geochemistry Department, Geological Survey of

Ethiopia, Addis Ababa, Ethiopia.

Irving, T. N. and Baragar, W. R. T. (1971) A guide to the chemical classification of the common rocks. Can. J. Earth Sci., 8, 523-548.

Kazmin, V. (1972) Geology of Ethiopia (Explanatory Note to Geological map of Ethiopia 1:2000,000). Imp. Eth. Gov., Min. Mines, Geological Survey of Ethiopia, Addis Ababa, 1-211.

Kazmin, V. (1979) Stratigraphy and correlation of Cenozoic volcanic rocks in Ethiopia. Ethiopian Institute of Geological Survey, Addis Ababa, Ethiopia, 106, 1-26.

Kazmin, V. (1980) Geodynamic control of rift volcanism. Geologische Rundschau 69, 757-769.

Le maitre, R.W., Bateman, P., Dudek, A., Kellar, J., Lameyre Le Bas, M.J., Sabine, P.A., Schmid, R., Sorensen, H., Streckeisen, A., Woolley, A.R. and Zanettin, B. (1989) A classification of igneous rocks and glossary of terms. Blackwell, Oxford.

Mohr, P.A. (1963) The Geology of Ethiopia. Addis Ababa University press, Addis Ababa, Ethiopia, 268.

Mohr, P.A. (1967) The Ethiopian Rift System. Bull. Geophys. Observatory. Addis Ababa. 11, 1-65.

Pearce, J.A. (1982) Trace element characteristics of lavas from destructive plate boundaries. In: Andesites and related rocks. (R.S. Thorpe ed.), 525-548.

Pik, R., Deniel, C., Coulon, C., Yirgu, G., Hoffmann, C. and Ayalew, D. (1998) The northwestern Ethiopian Plateau flood basalts: classification and spatial distribution of magma types. J. Volcanol. Geothem. Res., 81, 91-111.

Pik, R., Deniel, C., Coulon, C., Yirgu, G., Hoffmann, C. and Ayalew, D. (1999) Isotopic and trace element signatures of Ethiopian flood basalts: evidence for plume-lithosphere interactions. Geochim. Cosmochim. Acta, 63, 2263-2279.

Seyid, G. and Haro, W. (2003) Tertiary-Quaternary Volcanic Rocks; Geology of Subsheets B, H and western half of Subsheet J, Bure Sheet; Regional Geology and Geochemistry Department, Geological Survey of Ethiopia, Addis Ababa, Ethiopia.

Stewart, K. and Rogers, N. (1996) Mantle plume and lithosphere contributions to basalts from southern Ethiopia. Earth Planet. Sci. Lett., 139, 195-211.

Sun, S.S. and McDonough, W.F. (1989) Chemical and isotopic systematics of oceanic basalts: implications for mantle composition and processes. In: Saunders A.D. and Norry M.J. (eds.), Magmatism in oceanic basins. Geol. Soc. London. Spec. Pub. 42, 313-345.

Taylor, S.R. and McLennan, S.M. (1981) The composition and evolution of the continental crust: rare earth element evidence from sedimentary rocks. Phil. Trans. R. Soc., A301, 381-399.

Tefera, M., Chernet, T. and Haro, W. (1996) Explanation to the Geological map of Ethiopia, 2nd (ed.) 1:2,000,000. Ethiopian Institute of Geological Surveys.

Vidal, P., Deniel, C., Vellutini, P.J., Piguet, P., Coulon, C., Vincent, J. and Audin, J. (1991) Changes of mantle sources in the course of a rift evolution: the Afar case. Geophys. Res. Lett., 18, 1913-1916.

White, R. and McKenzie, D. (1989) Magmatism at Rift Zones: The Generation of volcanic Continental Margins and Flood Basalts. J. Geophys. Res., 94, 7685-7729.

Worku, A. and Woldu, A. (2003) Geology of sub-sheet R and X (Bure, NC37-5). Regional Geology and Geochemistry Department, Geological Survey of Ethiopia, Addis Ababa, Ethiopia.

Zanetiin, B., Justin-Visentin, E., Nicoletti, M. and Piccirilo, E. M. (1980a) Correlation among Ethiopian volcanic formations with special references to the Chronological and stratigraphic problems of the "Trap Series" in Geodynamic Evolution of the afro-Arabian Rift system. Accod. Naz. Dei. Lencei, Roma, 47, 231-252.